J Clin Immunol (2012) 32:611–621
DOI 10.1007/s10875-011-9635-2

The Role of Innate Cells Is Coupled to a Th1-Polarized Immune Response in Pediatric Nonalcoholic Steatohepatitis

Nazarena E. Ferreyra Solari · María Eugenia Inzaugarat · Placida Baz · Elena De Matteo · Carol Lezama · Marcela Galoppo · Cristina Galoppo · Alejandra C. Cherñavsky

Received: 7 October 2011 / Accepted: 8 December 2011 / Published online: 7 January 2012

Abstract
Background Nonalcoholic steatohepatitis (NASH) is a chronic inflammatory liver disease influenced by risk factors for the metabolic syndrome. In adult patients, NASH is associated with an altered phenotype and functionality of peripheral immune cells, the recruitment of leukocytes and intrahepatic activation, and an exacerbated production of reactive oxygen species (ROS) and cytokines. It remains unclear if the previously described differences between pediatric and adult nonalcoholic fatty liver diseases also reflect differences in their pathogenesis.
Aims We aimed to investigate the phenotype and functionality of circulating immune cells and the potential contribution of liver infiltrating leukocytes to the immunological imbalance in pediatric NASH.
Results By a real-time PCR-based analysis of cytokines and immunohistochemical staining of liver biopsies, we demonstrated that the hepatic microenvironment is dominated by interferon-gamma (IFN-γ) but not interleukin-4 and is infiltrated by a higher number of $CD8^+$ cells in pediatric NASH. The number of infiltrating neutrophils positively correlated with ROS generation by peripheral polymorphonuclear cells. By a flow cytometric analysis of peripheral blood lymphocytes, a distinctive increase in $CD8^+$ CD45RO and $CD8^+$ CD45RA subpopulations and an increased production of IFN-γ by $CD4^+$ and $CD8^+$ cells were shown. The production of ROS following PMA stimulation was augmented in circulating neutrophils but not in monocytes.
Conclusion In sum, the distinctive phenotype and functionality of infiltrating and circulating cells suggest that the role of innate cells is coupled to a Th1-polarized immune response in pediatric NASH.

Keywords Memory and naive T cell subsets · polymorphonuclear cells · oxidative stress · Th1/Th2 cytokines · pediatric NASH

Introduction

The spectrum of nonalcoholic fatty liver diseases (NAFLD) ranges from hepatic steatosis (simple fatty liver) to nonalcoholic steatohepatitis (NASH), which is its more progressive form, to advanced fibrosis and cirrhosis [1, 2]. NASH is histologically characterized by the presence of hepatic steatosis, ballooning, cell damage, and a mild portal and lobular infiltration of a small number of lymphocytes and polymorphonuclear leukocytes [3, 4]. The progression of NAFLD is explained by the "two-hit" hypothesis [5]. According to this hypothesis, an excessive accumulation of fat within hepatocytes represents the first hit [6]. This condition is supposed to augment the sensitivity to second multiple hits given by the complex interactions between liver resident cells, inflammatory mediators, and reactive

Nazarena E Ferreyra Solari and María Eugenia Inzaugarat contributed equally to this work.

N. E. Ferreyra Solari · M. E. Inzaugarat · P. Baz · A. C. Cherñavsky (✉)
Laboratorio de Inmunogenética, Hospital de Clínicas "José de San Martín", Universidad de Buenos Aires,
Av. Córdoba 2351, 3er piso,
CP1120, Buenos Aires, Argentina
e-mail: accher@fibertel.com.ar

E. De Matteo
Servicio de Patología, Hospital de Niños "Dr. R. Gutierrez", Universidad de Buenos Aires,
Buenos Aires, Argentina

C. Lezama · M. Galoppo · C. Galoppo
Unidad de Hepatología, Hospital de Niños "Dr. Ricardo Gutiérrez", Universidad de Buenos Aires,
Buenos Aires, Argentina

oxygen species (ROS) leading to cell death, inflammation, and fibrosis [7, 8]. NAFLD is also influenced by the presence of risk factors for the metabolic syndrome (MetS) with insulin resistance as a well-identified etiological factor [9]. The prevalence of NAFLD increases with age [10, 11] probably due to the aging process, increases in the incidence of the MetS, and modifications in the liver function [12]. Bacterial translocation allows the transfer of danger molecules into the liver of patients with NASH and promotes the activation of the innate immune response with expansion of the adaptive branch leading to the rupture of liver immune homeostasis [13]. Kupffer cells are critically involved during the progression of NAFLD either by a deficient supply of pro-inflammatory cytokines, chemokines and ROS, or by an excessive recruitment of cytotoxic effector cells such as lymphocytes and neutrophils [14, 15].

The presence of by-products of lipid peroxidation generated by local intrahepatic oxidative stress in NASH can exacerbate the influx of inflammatory cells supporting the progression of the disease [16, 17]. The histopathology of the liver in pediatric NAFLD has several distinct characteristics rarely seen in adults, but it remains unclear whether differences with age reflect differences in the pathogenesis of NAFLD [18]. The local infiltration of the liver with neutrophils [19] and the prevalence of $CD8^+$ cells with a minor component of natural killer and natural killer T cells [20] were described in adults with NASH. However, immunohistochemical studies were not performed in children.

The break of liver immune homeostasis is usually accompanied by changes in the frequency and/or in the functionality of peripheral T cell subpopulations [21, 22]. We have recently demonstrated the presence of an altered phenotype and functionality of circulating immune cells in adult patients with NASH [23].

The present study was designed to investigate the phenotypic characteristics and the functionality of circulating cells in pediatric NASH and the potential contribution of liver infiltrating lymphocytes and polymorphonuclear (PMN) cells to an immunological imbalance. To this end, we evaluated the frequencies of naive/memory CD4 and CD8 T cells, its Th1/Th2 commitment, and the generation of ROS by monocytes and neutrophils at the periphery, as well as liver infiltrating mononuclear (MN) cells, neutrophils, interferon gamma (IFN)-γ and interleukin (IL)-4 expression at the local compartment.

Material and Methods

Subjects

Fifteen pediatric patients with NASH (<15 years) from the Hepatology Unit of the Children's Hospital "Dr. Ricardo Gutiérrez" were enrolled. The decision to biopsy was made by a pediatric hepatologist, and the biopsy was usually done in view of abnormal transaminases and/or hepatomegaly. The diagnosis of NASH was based on the following criteria: (1) absence of other causes of liver disease, (2) exclusion of alcohol intake on history in adolescents, and (3) typical characteristic features of NASH in the liver biopsy including macrovesicular steatosis and lobular inflammation together with ballooning degeneration [24, 25]. Blood was taken on the day of diagnostic liver biopsy. Thirty age-matched [median age 12 years (range 6–18)] metabolically healthy individuals coming from the Clinical Hospital "José de San Martin" were included as controls in experiments using blood samples, and none of the controls underwent liver biopsy. Controls had not used medications and their body mass index (BMI) was appropriated for normal weight [26]. All subjects were informed of the aim of the study and gave their written informed consent. The study was approved by the respective local ethics committees informed of internationally endorsed standards for the application of the Helsinki Declaration. A clinical evaluation including anthropometric data, ultrasonography, and laboratory tests including liver enzymes aspartate aminotransferase (AST) and alanine aminotransferase (ALT), homeostasis model assessment (HOMA), triglycerides, and cholesterol were performed to all patients.

Histologic Analysis

The histologic diagnosis was established using hematoxylin and eosin (H&E) and Masson's trichrome stain of formalin-fixed paraffin-embedded liver samples and according to the nonalcoholic fatty liver disease scoring system. Slides from all biopsies were examined by two pathologists that scored the liver histology by using previously published criteria [24]. Activity grade was semi-quantitatively assessed using an eight-point scale: 0–3 (steatosis), + 0–3 (lobular inflammation), and + 0–2 (ballooning). Fibrosis stage was measured using a five-point scale.

Analysis of Polymorphonuclear Cells in Liver Infiltration

The presence of PMN cells was determined according to the size and shape of infiltrating cells. Neutrophils were counted with use of a Nikon microscope at a high magnification (×400), in five randomly chosen fields for each sample. At the portal tracts, the percentage of PMN cells out of 150 total leukocytes on average was assessed.

Immunochemistry

Primary monoclonal antibodies (mAbs) used to perform inmunostaining were anti-CD4 (IgG1), anti-CD20 (IgG2a), and anti-CD8 (IgG2b) (Dako, Carpinteria, CA, USA). Negative controls omitted primary antibodies. Briefly, 5-μm

sections of paraffin-embedded tissues were deparaffinized and rehydrated, and endogenous peroxidase activity was blocked with methanol–3% H_2O_2 and preincubated with diluted normal horse serum (Vector Laboratories, Burlingame, CA, USA). The CD20 antigen detection required a previous treatment in a microwave oven with sodium citrate buffer pH 6.0 and CD4 and CD8 antigens with ethylene diamine tetra-acetate pH 8.0 (EDTA). The CD20 antibody was diluted 1:150; CD4 1:5 and CD8 1:10 in phosphate-buffered saline (PBS) and incubated at 4°C overnight. Biotinylated antibodies and horseradish peroxidase-conjugated avidin biotin complex (ABC kit Elite, Vectastain® and 3,3′ diaminobenzidine substrate kit (Vector Laboratories) were used. Sections were counterstained with 10% Harris's hematoxylin. Stained cells at portal tracts were quantified at high magnification (×400) in five randomly chosen fields on average, and the percentage of positive cells out of total leukocytes was assessed.

Quantitative Polymerase Chain Reaction

Control liver tissues were obtained from cadaveric donors [median age 16 years (range 7–30)] by agreement with the Central Unique National Institute Coordinator of Ablation and Implant. All had normal transaminase values at death. After collection, both liver biopsies from patients with NASH and control tissues were immediately submerged in 1 ml of TRIZOL® reagent (GIBCO BRL, Life Technologies Inc., Grand Island, NY, USA) and stored at −70°C. Total RNA was isolated from tissues according to the protocol provided by the manufacturer. Reverse transcription was carried out by using the SuperScript® First-Strand Synthesis System for reverse transcriptase-PCR Kit (Invitrogen, Life Technologies, Carlsbad, CA, USA) and oligodT primers. Messenger RNA levels for IFN-γ, IL-4, and β-actin were determined by real-time PCR using a Stratagene Mx3005P® 4.1 Real-Time PCR system (Amersham Biosciences, USA). All reactions were performed in a volume of 25 μl using FastStart SYBR Green I MasterMix (Roche Applied Science, Indianapolis, USA) and Platinum® Taq DNA polymerase (Invitrogen). All primers were designed to span an intron of the genomic sequence. The forward and reverse primers (FP and RP) are as follows: β-actin FP and RP-5′ ATGGGTCAGAAGGATTCCTATGTG-3′ and 5′-CTTCATGAGGTAGTCAGTCAGGTC-3′; IFN-γ FP and RP-5′-TGGAAAGAGGAGAGTGACAG-3′ and 5′-ATTCATGTCTTCCTTGATGG-3′; and IL-4 FP and RP-5′-ACTGCACAGCAGTTCCACAG-3′and 5′-CTCTGGTTGGCTTCCTTCAC-3′. PCR conditions for gene amplification were a 10-min 95°C enzyme activation step followed by 40 cycles of 95°C for 30 s, 60°C for 60 s, and 72°C for 60 s. The expression of IFN-γ and IL-4 genes was normalized to β-actin content.

Reagents

Ficoll-Hypaque was purchased from Pharmacia Biotech (Uppsala, Sweden). RPMI 1640 medium was obtained from Life Technologies (Gaithersburg, MD, USA). Gentamicin, glutamine, gelatin, ionomycin, phorbol myristate acetate (PMA), brefeldin A, and 2′7′-dichlorofluorescin diacetate (DCFH-DA) were purchased from Sigma Chemical Co. (Saint Louis, MO, USA). DCFH-DA was made up daily by dissolving in PBS glucose containing 5 mM glucose, 0.1% gelatin, and 10% methanol (PBSg). The stock solution of PMA was prepared in dimethyl sulfoxide at 25 μg/ml and stored at −20°C. The mAbs for flow cytometry, the fixation kit, and the permeabilization buffer for intracitoplasmatic staining were purchased from Becton-Dickinson (BD) (Mountain View, CA, USA).

Cell Isolation Procedures

Blood samples were collected by venous puncture in heparin at the time of diagnosis and immediately processed to obtain MN cells and neutrophils. Peripheral blood mononuclear cells (PBMC) were prepared by Ficoll-Hypaque density gradient centrifugation at 2,000 rpm at room temperature for 20 min. PBMC were washed twice in PBS, counted, and resuspended in RPMI 1640 10% fetal bovine serum, 2 mmol/L-glutamine, and 50 μg/ml gentamicin. For neutrophil assays, 10 ml of lysis buffer containing 0.15 M ammonium chloride, 0.02 M sodium bicarbonate, and 1 mM EDTA was added to propylene tubes, and 1 ml of whole blood was then added to each tube. Tubes were mixed by inversion for 10 min and spun at 1,200 rpm for 10 min. Total leukocytes were washed twice in PBS and resuspended in RPMI 1640 to yield a final concentration of 10^6 cells/ml.

Monoclonal Antibodies and Cell Surface Staining

The following IgG1 isotype mAbs conjugated with fluorescein isothiocyanate (FITC) or peridinin–chlorophyll–protein complex (PerCP) were used for flow cytometry analysis of PBMC: CD4 (Leu3a/PerCP), CD8 (Leu2/PerCP), CD45RA (HI100/FITC), and CD45RO (UCHL1/FITC). The same IgG1's isotype mAbs (G1CL-FITC) were used at the same concentration to control for nonspecific binding. After incubation with surface-specific mAbs at 4°C for 30 min, PBMC were washed and resuspended in PBS.

Monoclonal Antibodies and Intracellular Cytokine Detection

PMBC were stimulated with 25 ng/ml of PMA and 1 mM ionomycin in the presence of 1 mM brefeldin A at 37°C for

4 h. After stimulation, cell surface staining was performed using anti-CD4 or anti-CD8 PerCP as describe above. After that, the cells were fixed at 4°C for 20 min using the fixation kit and then washed with the permeabilization buffer. PE-conjugated anti-IFN-γ or anti-IL-4 or the corresponding isotypes were added to the cells and incubated at 4°C for 40 min in the presence of 50 μl of permeabilization buffer.

DCFH-DA Oxidation

PBMC or total leukocytes (10^6 cells/ml) were incubated with 10 μl of DCFH-DA in PBSg, yielding a final concentration of 5 μM with shaking at 37°C for 15 min. After two washes with PBS, cell stimulation was initiated with the addition of 100 ng/ml of PMA at 37°C for 20 min (for PMN cells) or 60 min (for monocytes). Basal ROS production by circulating cells was evaluated by analyzing saline-treated preparations. Following stimulation, PBMC were incubated with anti-CD14 (M5E2/PE) for 20 min at 4°C.

Flow Cytometric Analysis

Gates were separately set on lymphocytes, monocytes, or neutrophils according to their forward scatter (FSC) and side scatter (SSC) properties and used to collect events from tubes stained with the control isotypes or the different fluorochrome-conjugated mAbs. For lymphocyte analysis, cells were gated on the basis of SSC and simultaneous CD4 (or CD8) expression. The expression of CD45RO and CD45RA isoforms was analyzed in the selected CD4 (or CD8) gates. For monocyte analysis, cells were gated in a FSC/SSC dot plot (region R1). Within R1, CD14-expressing cells were further gated in the SSC/FL2-PE dot plot (R2). Finally, the R2 population was analyzed regarding its DCF fluorescence in an FL1-FITC histogram. Neutrophils were gated in a FSC/SSC dot plot and then analyzed for their DCF fluorescence. Isotype-matched negative control mAbs were used in all cases to assess background fluorescence intensity. Acquisition and analysis were performed on a FACSCalibur flow cytometer (BD) using the FlowJo software version 5.7.2.

Statistical Analysis

GraphPad Prism© software (GraphPad, San Diego, CA, USA) was used for all analysis. Normality was assessed by the Kolmogorov–Smirnov test. The Mann–Whitney *U* test or Kruskal–Wallis variance analysis was used to compare data between groups. Values were expressed as median values, lower and upper quartiles as corresponding. Spearman's rank correlation coefficients were used to test the association between nonparametric parameters measured in patients with NASH. The level of significance was fixed in all cases at $p<0.05$.

Results

Demographical Features and Clinical, Laboratory, and Histological Parameters in Patients with NASH

A complete characterization of the patients enrolled in the study is shown in Table I. Patients' median age was 11 years (range 8 to 15), and gender distribution was 53% of males and 47% of females. All NASH patients showed elevated BMI according to Cole's BMI cutoff points [26], being 73% obese and 27% overweight. The control's median age was 7 years (range 6 to 15). All control individuals showed normal BMI for age and sex. The AST and ALT levels were elevated in 33% and 67% of the patients, respectively. An abnormal lipid profile (increased total cholesterol and/or triglycerides) was found in 80% of patients and the HOMA values were found elevated in 60% of patients with NASH. The degree of hepatic steatosis was generally severe (80%), mild lobular inflammation was observed in about 60% of patients while inflammation was moderate in the remaining 40%. None of the patients showed a severe pattern of inflammation. A mild degree of ballooned hepatocytes was exhibited by 67% of patients while 33% have a moderate degree. Eighty-six percent of patients with NASH demonstrated signs of fibrosis with bridging fibrosis (60%), portal and periportal fibrosis (13%), and portal fibrosis (13%). Portal inflammation was seen in all patients with either mild (73.33%) or moderate (20%) characteristics. Only one patient showed signs of severe portal inflammation (6.66%).

Analysis of Liver Biopsies

We have previously described the distribution of MN cell subpopulations in portal tracts and periportal and lobular areas of the liver [27]. Herein, the immunophenotype of MN cells infiltrating the portal tracts was characterized by immunohistochemistry and quantified in liver biopsies from ten patients with NASH. The statistical analysis showed an over than three times greater median value for $CD8^+$ cells in comparison to both $CD4^+$ and $CD20^+$ values (Fig. 1).

Interferon-γ and IL-4 mRNA expression was assessed in four out of ten biopsy samples available. For comparison, CL from 14 donors was analyzed. Biopsies from patients showed an increased expression of IFN-γ [1.98 (1.47–40.11) vs. 0.38 (0.08–0.53), $p=0.01$, two-tailed Mann–Whitney *U* test] but not of IL-4 [0.22 (0.03–0.43), p=ns, two-tailed Mann–Whitney *U* test] (data not shown).

Table I Individual characterization of patients with NASH

Patient	Gender, age	BMI		HOMA	Serum transaminases		Lipid profile		Histological characteristics				
					AST	ALT	TC	TG	St	Inf	Ball	Fib	AG
1	M, 13	26.9	Ob	1.01	61	109	165	254	3	1	1	3	5
2	F, 11	24.0	Over	4.40	43	85	144	111	2	1	2	1c	5
3	F,11	25.4	Ob	3.39	21	16	133	236	2	1	1	3	4
4	M, 15	30.3	Ob	4.20	20	13	195	62	1	1	1	2	3
5	F, 15	29.0	Over	7.00	41	74	169	99	3	1	1	3	5
6	F, 9	22.7	Ob	3.60	26	56	111	101	3	2	1	3	6
7	F, 10	25.3	Over	3.70	24	85	147	117	3	2	1	3	6
8	F, 10	28.2	Ob	2.30	55	80	146	127	3	2	1	3	6
9	F, 12	25.6	Ob	4.50	24	27	172	137	3	1	2	3	5
10	M, 13	25.1	Ob	1.39	25	28	145	66	3	1	1	0	5
11	M, 10	27.2	Ob	3.50	78	18	207	78	3	2	1	2	6
12	M, 12	25.5	Over	3.70	83	157	138	91	3	1	2	0	6
13	M, 8	31.3	Ob	5.43	42	57	201	50	3	2	2	7	3
14	M, 10	31.4	Ob	2.10	44	76	106	47	3	1	1	1c	5
15	M, 9	26.1	Ob	7.79	125	171	99	76	3	1	2	6	3

AG: 0–3 (St), +0–3 (Inf), and +0–2 (Ball). To determine whether patients showed overweight or obesity, Cole's BMI cutoff points were used [26]. HOMA cutoff value was set in 3.5. Normal ALT and AST levels are ≤32 and ≤48 IU/l, respectively. The reference ranges for TC and TG are <181 and <119 mg/dl, respectively. Steatosis score: 0 (5% cells), 1 (5–33%), 2 (33–66%), and 3 (66%). Inflammation score: 0 (0 foci), 1 (2 foci), 2 (2–4 foci), and 3 (4 foci). Ballooning score: 0 (none), 1 (few balloon cells), and 2 (many cells/prominent balloon cells). Fibrosis stage: 0 (none), 1a, b [mild (a)/moderate (b)] zone 3 perisinusoidal fibrosis and 1c (mild/moderate only portal fibrosis), 2 (zone 3 and portal/periportal fibrosis), 3 (bridging fibrosis), and 4 (cirrhosis)

BMI body mass index (kilogram per square meter), *Ob* obesity, *Over* overweight, *HOMA* homeostasis model assessment, *AST* (international units per liter) aspartate aminotransferases, *ALT* (international units per liter) alanine aminotransferases, *TC* (milligram per deciliter) total cholesterol, TG (milligram per deciliter) triglycerides, *St* steatosis, *Inf* lobular inflammation, *Ball* ballooning, *Fib* fibrosis, *AG* activity grade

Analysis of Lymphocytes at the Peripheral Compartment

The expression of CD45RA and CD45RO isoforms of CD45 antigen in the population of $CD4^+$ and $CD8^+$ is shown in Fig. 2. Within the CD4 compartment, the proportions of CD45RA and CD45RO were similar in patients and controls. In contrast, the proportions of both naive and memory cells within the CD8 compartment were higher in patients than controls [68.50 (57.90–73.10), p=0.03 and 22.00 (18.30–25.00), p=0.02, respectively].

The commitment to a Th1, Th2, or cytotoxic cell obtained at priming by circulating lymphocytes was assessed after stimulating PBMC under neutral conditions performing an analysis of intracellular cytokine production. The synthesis of IFN- γwas examined within both $CD4^+$ and $CD8^+$ subpopulations whereas IL-4 production was only analyzed within $CD4^+$ subpopulation. Among metabolically healthy controls, percentages of producer cells below 10% were observed in all cases. Patients with NASH showed 2.5 and 4.2 times greater median values for $CD4^+$ and $CD8^+$ cells secreting IFN-γ, respectively, compared to controls [14.27 (11.84–16.29) vs. 5.69 (5.58–9.86), p= 0.008 and 24.97 (17.35–31.64) vs. 7.84 (5.25–8.07), p= 0.002]. In contrast, similar median percentage values for $CD4^+$ cells secreting IL-4 were found in patients and controls (Fig. 3).

Analysis of Cellular Components of the Innate Immune Response at the Local and Peripheral Compartments

At the local compartment, neutrophils were mainly observed at portal tracts and also scattered at lobular areas by histological examination of liver biopsies (Fig. 4, upper left panel). On the other hand, we compared the DCF fluorescent signals generated by circulating neutrophils based on a stimulation index (SI) in patients and controls. The SI was defined by the ratio between the mean channel fluorescence intensities of PMA-stimulated and unstimulated neutrophils. A higher amount of ROS was produced by neutrophils from patients with NASH compared with controls as evidenced by their increased median SI values [15.41 (7.90–19.07) vs. 3.60 (3.09–5.17), p=0.001] (Fig. 4, lower left panel). By Spearman's rank correlation coefficient analysis, we found a positive correlation between the percentage of infiltrating neutrophils and the SI for circulating neutrophils (r=0.83, p=0.015) (Fig. 4, lower right panel). We also evaluated the

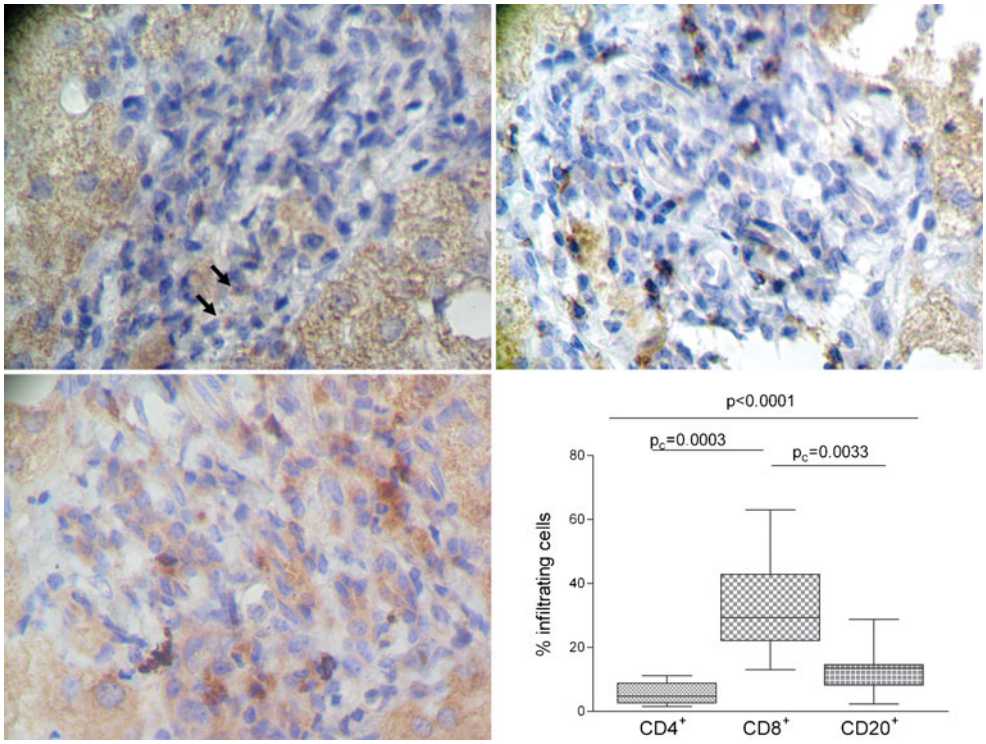

Fig. 1 Immunophenotype of liver infiltrating mononuclear cells. Photomicrographs of immunostained paraffin-embedded sections of liver tissue from a representative patient with NASH are shown. *Upper left*: $CD4^+$ cells; *upper right*: $CD8^+$ cells; *lower left*: $CD20^+$ cells. Original magnification ×400. Patients 1–6 and 12–15 were studied (Table I). The main observations are the prevalence of $CD8^+$ infiltrating cells with small numbers of $CD4^+$ and $CD20^+$ cells. *Lower right*: the compiled data from ten patients were analyzed by nonparametric Kruskal–Wallis variance analysis and Bonferroni's post test. The *box and whiskers* show nonparametric statistics: median, lower and upper quartiles, and confidence interval around the median. The percentage of $CD8^+$ infiltrating cells was higher than both $CD4^+$ and $CD20^+$ in liver biopsies

DCF fluorescent signals generated by circulating monocytes after PMA stimulation. By this functional study based on ROS generation, monocytes showed similar median SI values in patients and controls [3.85 (2.82–6.51) vs. 2.88 (1.65–3.37), $p=0.07$] (data not shown).

Discussion

In the present study, we demonstrated that the local microenvironment in pediatric NASH is dominated by the presence of IFN-γ, with a predominance of $CD8^+$ cells over $CD4^+$ and $CD20^+$ subpopulations and a high number of infiltrating neutrophils in correlation with ROS generation by peripheral neutrophils. Also, alterations in the phenotype and functionality of circulating lymphocytes and neutrophils compared with age-matched controls were shown. Concerning peripheral blood lymphocytes, we described the simultaneous increase in both $CD8^+$ CD45RO and $CD8^+$ CD45RA subpopulations and an increased percentage of $CD4^+$ and $CD8^+$ cells producing IFN-γ. Regarding neutrophils, an augmented production of ROS following stimulation with PMA was described in patients with NASH. Through the same functional study based on ROS generation, oxygen metabolism of circulating monocytes was similar to controls.

The liver contains a low number of $CD4^+$ and $CD8^+$ cells in portal tracts and scattered through the parenchyma [28] but chronic liver injury is usually associated with inflammatory infiltrates [27, 29]. The predominance of $CD8^+$ infiltrating cells herein described and the increased expression of IFN-γ strongly suggest the presence of a local cytotoxic response in the liver of pediatric patients with NASH.

Naive and memory T cells can be phenotypically distinguished based on the expression of CD45 antigen isoforms. Whereas memory T cells display CD45RO after the stimulation by antigens, naive T cells carry CD45RA [30, 31]. The expression of CD45 isoforms on the surface of LT helpers and cytotoxic cells was extensively studied in healthy individuals [32, 33] and also searching for the establishment of the immunologic background in a large

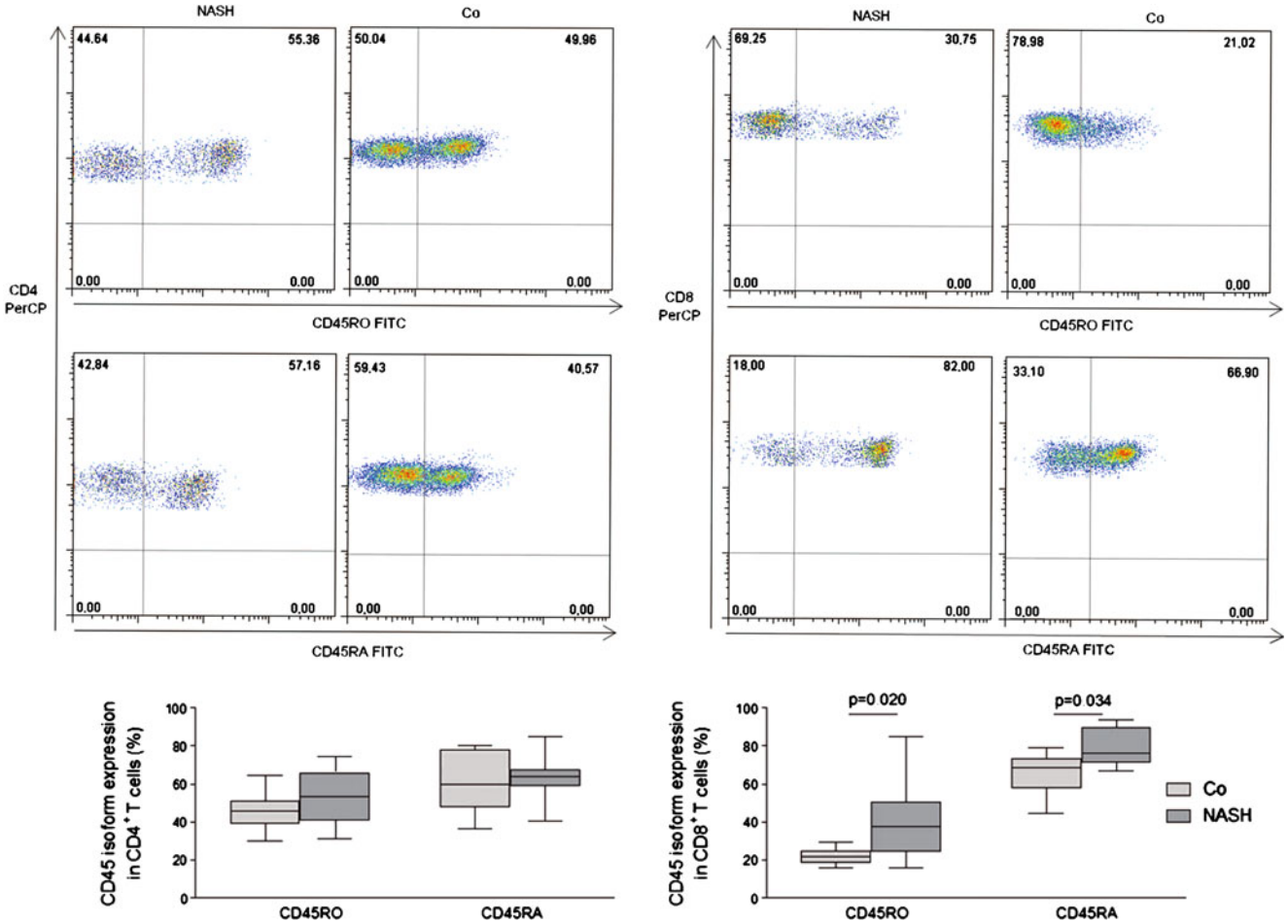

Fig. 2 Expression of CD45RA and CD45RO isoforms in $CD4^+$ and $CD8^+$ circulating cells. Patients 1–6 (CD4 compartment) and 1–6, 12, 13, and 14 (CD8 compartment) were studied (Table I). *Upper panel*: representative dot plots of CD45R0 and CD45RA expression in $CD4^+$ (*left*) and $CD8^+$ (*right*) circulating T cells in a patient with NASH (*NASH*) and a control (*Co*), respectively. *Lower panel*: the relative proportions of both $CD4^+$ CD45RO and $CD4^+$ CD45RA to total T cells, respectively, were similar in patients (NASH, $n=6$) and controls (Co, $n=10$). Conversely, the relative proportions of $CD8^+$ CD45RO and $CD8^+$ CD45RA to total T cells, respectively, were higher in patients ($n=10$) than controls ($n=10$). The *box and whiskers* show nonparametric statistics: median, lower and upper quartiles, and confidence interval around the median. A two-tailed Mann–Whitney *U* test was used to determine significant differences between the two groups. A value of $p<0.05$ was considered statistically significant

range of diseases. For instance, an altered profile of CD45 isoform expression has been associated with metabolic diseases such as hypothyroidism and diabetes type 2 [21] and many chronic liver diseases such as infantile cholestasis and hepatitis C [34]. Moreover, we have recently described a differential distribution of CD45 isoforms among both $CD4^+$ and $CD8^+$ T cells in adults with NASH [23]. In pediatric patients, however, whereas CD45RO and CD45RA subpopulations were similarly distributed among circulating $CD4^+$, both $CD8^+$ CD45RO and $CD8^+$ CD45RA subpopulations were found simultaneously increased in patients. Not only the mitogenic stimulation of naive T cells induces the co-expression of surface CD45RO and CD45RA markers, but there is also a dual expression of CD45 isoforms during the conversion from a CD45RO to a CD45RA phenotype [35]. Hence, an increase of dual expressing (CD45RO/CD45RA) in the pool of circulating CD8 cells might explain the simultaneous increases observed in both $CD8^+$ CD45RO and $CD8^+$ CD45RA subpopulations in our patients. On the other hand, the greater frequency of circulating $CD8^+$ CD45RA cells in patients with NASH might correspond to CD8 T memory cells CD45RA-positive denominated "effector memory RA" [36]. Each one of both circumstances refers to a greater pool of CD8 T cells undergoing activation in patients than controls.

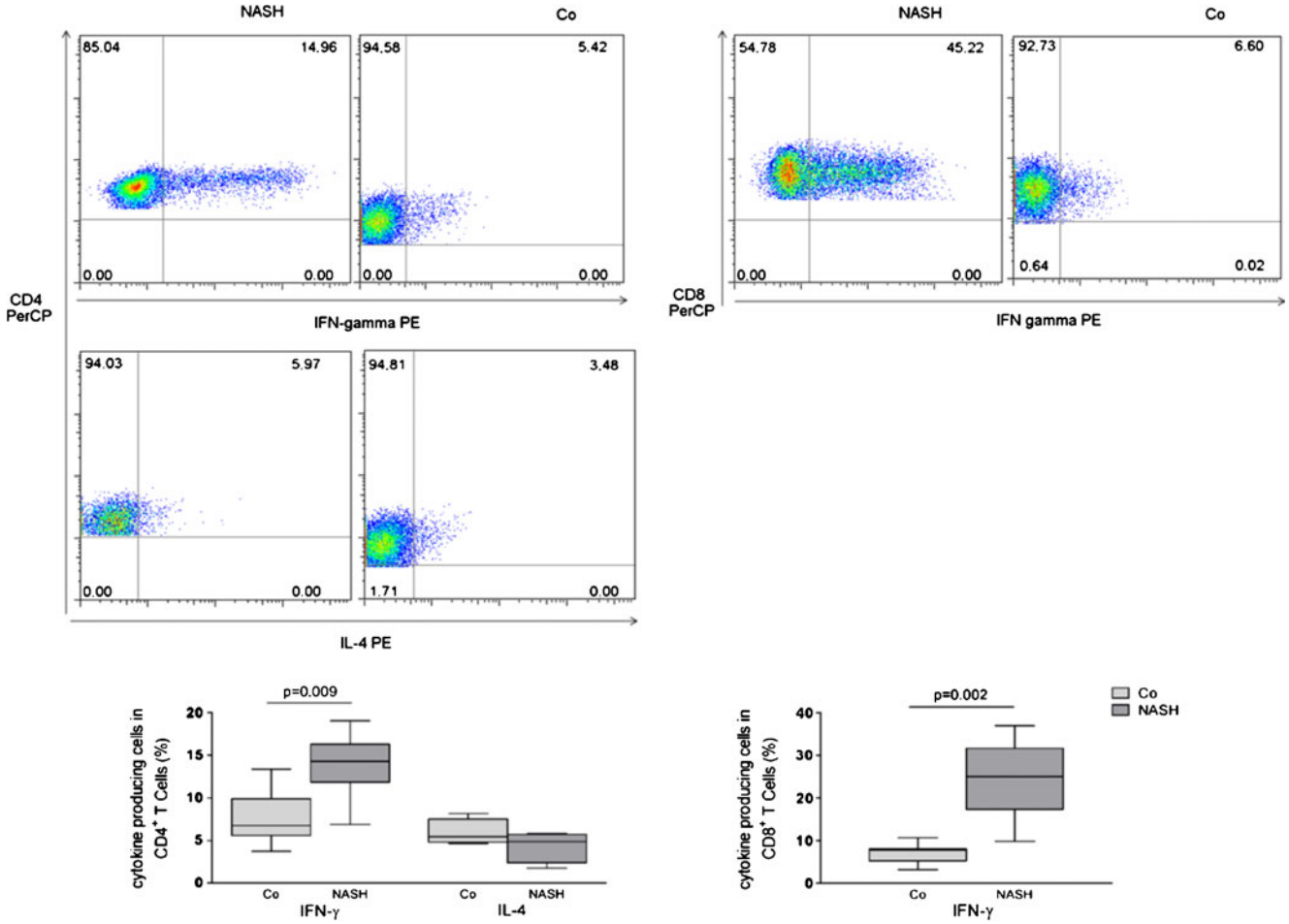

Fig. 3 Percentage of IFN-γ and IL-4 producing $CD4^+$ and $CD8^+$ cells in peripheral blood. Patients 10, 11, 12, 13, 14, and 15 (Table I) were studied. Cells were gated on CD4 or CD8 vs. side scatter dot plots. *Upper panel*: representative dot plots of $CD4^+$ (*right*) and $CD8^+$ (*left*) cells showing intracellular IFN-γ and IL-4 in a patient with NASH (*NASH*) and a control (*Co*). The percentages of IFN-γ producing/total $CD4^+$ and IFN-γ producing/total $CD8^+$ cells, respectively, were higher in patients (NASH, $n=6$) compared to controls (Co, $n=5$). No differences were found between both groups regarding IL-4 producing $CD4^+$ cells. The *box and whiskers* show nonparametric statistics: median, lower and upper quartiles, and confidence interval around the median. A two-tailed Mann–Whitney *U* test was used to determine significant differences between the two groups. A value of $p<0.050$ was considered statistically significant

As memory cells retain the Th1, Th2, or cytotoxic commitment that was imprinted at priming when stimulated under neutral conditions [37], in the present study, PBMC were incubated with PMA and ionomycin to characterize the intracellular expression of IFN-γ and IL-4. As described in adults [23], increased percentages of circulating $CD4^+$ cells retaining a Th1 phenotype as well as $CD8^+$ cells retaining a cytotoxic phenotype were found in pediatric patients. The increased percentages of both circulating $CD4^+$ and $CD8^+$ cells expressing IFN-γ in patients with NASH agree with the suggested presence of a local cytotoxic response in the liver. IL-4 production, on the other hand, appeared to be related to a constitutional feature of the investigated individuals.

Different experimental evidences point to an important role of IFN-γ in hepatic damage [38, 39]. Our present data concerning the Th1 phenotype at the peripheral CD4 compartment and the increased expression of IFN-γ in the liver of patients with NASH allow us to consider NASH as a Th1-polarized disease.

The previously observed infiltration of neutrophils into the liver and the augmented production of ROS following stimulation with PMA in adult patients with NASH [19, 23] led us to consider the probable involvement of these cells in pediatric NASH. The greater SI observed in our patients might be due to a primed status of circulating neutrophils by which it readily gets activated upon subsequent stimulation with PMA [40]. On

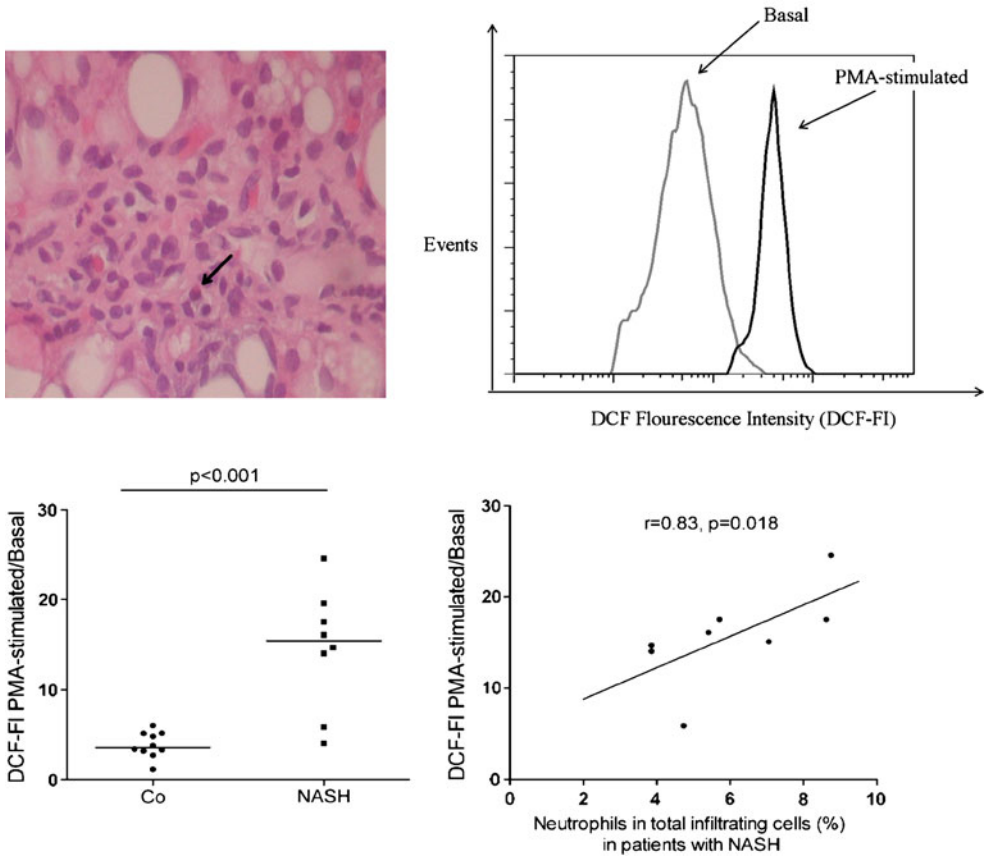

Fig. 4 Stimulation index in peripheral blood neutrophils after challenge of total leukocytes with PMA. Patients 7, 9, 10, 11, 12, 13, 14, and 15 (Table I) were studied. *Upper panel*: H&E staining showed the presence of PMN cells in a representative liver biopsy of a patient with NASH (*left*); total leukocytes preincubated with DCFH-DA were stimulated with PMA (100 ng/ml) for 20 min. A gate was made for the neutrophil subpopulation in a FSC vs. SSC dot plot and then analyzed for DCF fluorescence intensity (*right*). *Lower panel*: SI for neutrophils was defined by the ratio between DCF fluorescence intensity (DCF-FI) in PMA-stimulated and unstimulated (basal) neutrophils. The SI were higher in patients (NASH, $n=8$) than controls (Co, $n=10$). *Horizontal bars* show the median values. A two-tailed Mann–Whitney *U* test was used to determine significant differences between the two groups. A value of $p<0.05$ was considered statistically significant (*left*). The positive correlation between the percentages of infiltrating neutrophils and the SI in peripheral neutrophils was demonstrated by Spearman's rank correlation coefficient test ($r=0.83$, $p=0.015$) (*right*)

the other hand, leptin up-regulates the expression of CD11b on neutrophils, an early marker of activation which is also involved in neutrophil localization at inflammatory sites [41]. As leptin is augmented in pediatric patients with NAFLD [42], the positive correlation between the number of infiltrating PMN neutrophils and ROS generation might reveal a link between a greater activation status of peripheral neutrophils and the recruitment of these cells to the liver. Even though leptin also activates monocytes [43], the present functional study based on ROS generation failed to reveal a monocyte inflammatory phenotype in pediatric patients, in agreement with our previous results in adult NASH [23]. We hypothesize that the result concerning circulating monocytes is not unexpected given that the production of IFN-γ by lymphocytes upon entering the liver might support the classic activation of intrahepatic macrophages [15].

Conclusions

We demonstrated a distinctive phenotype of circulating cells that points to a greater pool of $CD8^+$ T cells undergoing activation in pediatric NASH. However, the functionality of lymphocytes, neutrophils, and monocytes did not differ from our previously reported observations in adult NASH. The role of innate cells in pediatric NASH is coupled to a Th1-polarized immune response.

References

1. Paschos P, Paletas K. Non alcoholic fatty liver disease and metabolic syndrome. Hippokratia. 2009;13:9–19.
2. Vuppalanchi R, Chalasani N. Non-alcoholic fatty liver disease and non-alcoholic steatohepatitis: past, present and future directions. J Gastrointestin Liver Dis. 2010;19:415–23.
3. Brunt EM. Pathology of nonalcoholic steatohepatitis. Hepatol Res. 2005;33:68–71.
4. Brunt EM. Histopathology of non-alcoholic fatty liver disease. Clin Liver Dis. 2005;13:533–44.
5. Day C, James OFW. Steatohepatitis: a tale of two "hits"? Gastroenterology. 1998;114:842–5.
6. Basaranoglu M, Kayacetin S, Yilmaz N, Kayacetin E, Tarcin O, Sonsuz A. Understanding mechanisms of the pathogenesis of nonalcoholic fatty liver disease. World J Gastroenterol. 2010;16:2223–6.
7. Fassio E, Alvarez E, Dominguez N, Landeira G, Longo C. Natural history of nonalcoholic steatohepatitis: a longitudinal study of repeat liver biopsies. Hepatology. 2004;40:820–6.
8. Jasen PML. Nonalcoholic steatohepatitis. J Med. 2004;62:217–24.
9. Pascale A, Pais R, Ratziu V. An overview of nonalcoholic steatohepatitis: past, present and future directions. J Gastrointestin Liver Dis. 2010;19:415–23.
10. Tominaga K, Fujimoto E, Suzuki K, Hayashi M, Ichikawa M, Inaba Y. Prevalence of non-alcoholic fatty liver disease in children and relationship to metabolic syndrome, insulin resistance, and waist circumference. Environ Health Prev Med. 2009;14:142–9.
11. Argo CK, Caldwell SH. Epidemiology and natural history of nonalcoholic steatohepatitis. Clin Liver Dis. 2009;13:511–31.
12. Frith J, Jones D, Newton J. Chronic liver disease in an ageing population. Age Ageing. 2009;38:11–8.
13. Singh R, Bullard J, Kalra M, Assefa S, Kaul AK, Vonfeldt K, et al. Status of bacterial colonization, Toll like receptor expression and nuclear factor-kappa B activation in normal and diseased human livers. Clin Immunol. 2011;138:41–9.
14. Jaeschke H, Gores GJ, Cederbaum AI, Hinson JÁ, Pessayre D, Lemasters JJ. Mechanisms of hepatotoxicity. Toxicol Sci. 2002;65:166–76.
15. Buffy G. Kupffer cells in non-alcoholic steatohepatitis: the emerging view. J Hepatol. 2009;51:212–23.
16. Seki S, Kitada T, Yamada T, Sakaguchi H, Nakatani K, Wakasa K. In situ detection of lipid peroxidation and oxidative DNA damage in non-alcoholic fatty liver diseases. J Hepatol. 2002;37:56–62.
17. Abdelmalek MF, Diehl AM. Mechanisms underlying nonalcoholic steatohepatitis. Drug Discov Today: Dis Mech. 2006;3:479–88.
18. Schwimmer JB, Behling C, Newbury R, Deutsch R, Nievergelt C, Schork NJ, Lavine JE. Histopathology of pediatric nonalcoholic fatty liver disease. Hepatology. 2005;42:641–9.
19. Rensen SS, Slaats S, Nijhuis J, Jans A, Bieghs V, Driessen A, Malle E, Greve JW, Buurman WA. Increased hepatic myeloperoxidase activity in obese subjects with nonalcoholic steatohepatitis. Am J Pathol. 2009;175:1473–82.
20. Adler M, Taylor S, Okebugwu K, Yee H, Fielding C, Fielding G, Poles M. Intrahepatic natural killer T cell populations are increased in human hepatic steatosis. World J Gastroenterol. 2011;17:1725–31.
21. Li QF, Li YP, Cheng PS. Peripheral T-lymphocyte subsets changes in patients with endocrine and metabolic diseases. Zhonghua Nei Ke Za Zhi. 1989;28:410–2.
22. Romo EM, Muñoz-Robles JA, Castillo-Rama M, Meneu JC, Moreno-Elola A, Perez-Saborido B, et al. Peripheral blood lymphocyte populations in end-stage liver diseases. J Clin Gastroenterol. 2007;41(7):713–21.
23. Inzaugarat ME, Ferreyra Solari NE, Billordo LA, Abecasis R, Gadano AC, Cherñavsky AC. Altered phenotype and functionality of circulating immune cells characterize adult patients with nonalcoholic steatohepatitis. J Clin Immunol. 2011;31:1120–30.
24. Kleiner DE, Brunt EM, Van Natta M, Behling C, Contos MJ, Cummings OW, Ferrell LD, Liu YC, Torbenson MS, Unalp-Arida A, Yeh M, McCullough AJ, Sanyal AJ. Design and validation of a histological scoring system for nonalcoholic fatty liver disease. Hepatology. 2005;41:1313–21.
25. Brunt EM, Janney CG, Di Bisceglie AM, Neuschwander-Tetri BA, Bacon BR. Nonalcoholic steatohepatitis: a proposal for grading and staging the histological lesions. Am J Gastroenterol. 1999;94:2467–74.
26. Cole TJ, Bellizzi MC, Flegal KM, Dietz WH. Establishing a standard definition for child overweight and obesity worldwide: international survey. BMJ. 2000;320:1–6.
27. De Basio MB, Periolo N, Avagnina A, Garcia de Davila MT, Ciocca M, Goñi J, de Mateeo E, Galoppo C, Cañero-Velasco MC, Fainboim H, Muñoz AE, Fainboim L, Cherñavsky AC. Liver infiltrating mononuclear cells in children with type 1 autoimmune hepatitis. J Clin Pathol. 2006;59:417–23.
28. Lalor PL, Shields P, et al. Recruitment of lymphocytes to the human liver. Immunol Cell Biol. 2002;80:52–64.
29. Lemmers A, Moreno C, Gustot T, et al. The interleukin-17 pathway is involved in human alcoholic liver disease. Hepatology. 2009;49:646–57.
30. Berard M, Tough DF. Qualitative differences between naïve and memory T cells. Immunology. 2002;106:127–38.
31. Linton JP, Haynes L, Tsui L, Zhang X, Swain S. From naive to effector—alterations with aging. Immunol Rev. 1997;160:9–18.
32. Kimmig S, Przybylski GK, Schmidt CA, Laurisch K, Mowes B, Radbruch A, Thiel A. Two subsets of naive T helper cells with distinct T cell receptor excision circle content in human adult peripheral blood. J Exp Med. 2002;195:789–94.
33. Richards SJ, Jones RA, Roberts BE, Patel D, Scott CS. Relationships between 2H4 (CD45RA) and UCHLl (CD45RO) expression by normal blood $CD4^+$ $CD8^-$, $CD4^-$ $CD8^+$, $CD4^-$ $CD8^{dim+}$, $CD3^+$ $CD4^-CD8^-$ and $CD3^-$ $CD4^-CD8^-$ lymphocytes. Clin Exp Immunol. 1990;81:149–55.
34. Socha P, Michalkiewicz J, Stachowski J, Pawlowska J, Jankowska I, Barth C, Socha J, Madalinski K. Deficiency of the expression of CD45RA isoform of CD45 common leukocyte antigen in CD4+ T lymphocytes in children with infantile cholestasis. Immunol Let. 2001;78:179–84.
35. Summers KL, O'Donnell JL, Hart DNJ. Co-expression of the CD45RA and CD45RO antigens on T lymphocytes in chronic arthritis. Clin Exp Immunol. 1994;97:39–44.
36. Hu X, Gu Y, Wang Y, Cong Y, Qu X, Xu C. Increased CD4+ and CD8+ effector memory T cells in patients with aplastic anemia. Annu Rev Immunol. 2004;22:745–63.
37. Messi M, Giacchetto I, Nagata K, Lanzavecchia A, Natoli G, Saluusto F. Memory and flexibility of cytokine gene expression as separable properties of human T(H)1 and T(H)2 lymphocytes. Nat Immunol. 2003;4:78–86.
38. Weng HL, Cai WM, Liu RH. Animal experiment and clinical study of effect of gamma-interferon on hepatic fibrosis. World J Gastroenterol. 2001;7:42–8.
39. Knight B, Lim R, Yeoh GC, Olynyk JK. Interferon-γ exacerbates liver damage, the hepatic progenitor cell response and fibrosis in a mouse model of chronic liver injury. J Hepatol. 2007;47:826–33.

40. Videm V, Strand E. Changes in neutrophil surface-receptor expression after stimulation with FMLP endotoxin, interleukin-8 and activated complement compared to degranulation. Scand J Immunol. 2004;59:25–33.
41. Zarkesh-Esfahani H, Pockley AG, Wu Z, Hellewell PG, Weetman AP, Ross RJ. Leptin indirectly activates human neutrophils via induction of TNF-alpha. J Immunol. 2004;172:1809–14.
42. Fitzpatrick E, Mitry RR, Quaglia A, Hussain MJ, DeBruyne R, Dhawan A. Serum levels of CK18 M30 and leptin are useful predictors of steatohepatitis and fibrosis in paediatric NAFLD. J Pediatr Gastroenterol Nutr. 2010;51:500–6.
43. Santos-Alvarez J, Goberna R, Sanchez-Margalet V. Human leptin stimulates proliferation and activation of human circulating monocytes. Cell Immunol. 1999;194:6–11.